Supplementary information for "Direct time-domain determination of electron-phonon coupling strengths in Chromium"

J. Wingert,[1,*] A. Singer,[1,2] S. K. K. Patel,[1,3] R. Kukreja,[1] Matthieu J. Verstraete,[4,5] Aldo H. Romero,[6] V. Uhlíř,[7,8] S. Festersen,[9] D. Zhu,[10] J. M. Glownia,[10] H. T. Lemke,[10] S. Nelson,[10] M. Kozina,[10] K. Rossnagel,[9] B. M. Murphy,[9,11] O. M. Magnussen,[9,11] E. E. Fullerton,[3] and O. G. Shpyrko[1]

[1]*Department of Physics, University of California, San Diego, La Jolla, California 92093, USA*
[2]*Present address: Department of Materials Science and Engineering, Cornell University, NY 14853, Ithaca*
[3]*Center for Memory and Recording Research, University of California, San Diego, La Jolla, California 92093, USA*
[4]*nanomat/Q-MAT/CESAM, Université de Liège, allée du 6 août, 19, B-4000 Liège, Belgium.*
[5]*European Theoretical Spectroscopy Facility www.etsf.eu*
[6]*Department of Physics and Astronomy, West Virginia University, Morgantown, WV 26505-6315, USA*
[7]*Center for Magnetic Recording Research, University of California, San Diego, La Jolla, California 92093, USA*
[8]*CEITEC BUT, Brno University of Technology, Purkyňova 123, 612 00 Brno, Czechia*
[9]*Institute for Experimental and Applied Physics, Kiel University, 24098 Kiel, Germany*
[10]*LCLS, SLAC National Accelerator Laboratory, Menlo Park, California 94025, USA*
[11]*Ruprecht Haensel Laboratory, Kiel University, 24098 Kiel, Germany*

(Dated: September 2019)

AB INITIO PARAMETERS FOR THE GROUND STATE

The electron phonon coupling was calculated using established methods based on density functional perturbation theory (DFPT [1]), as implemented in the ABINIT software package[2]. The ground state was described using a norm conserving pseudopotential following the Hamann ONCVPSP scheme [3] distributed on the pseudo-dojo web site [4], a plane wave kinetic energy cutoff of 50 Hartree, and the PBE exchange correlation functional[5] (with comparisons to LDA as well). The ground state potential residual was converged below 1.e-16, intermediate wavefunction residuals below 1.e-20.

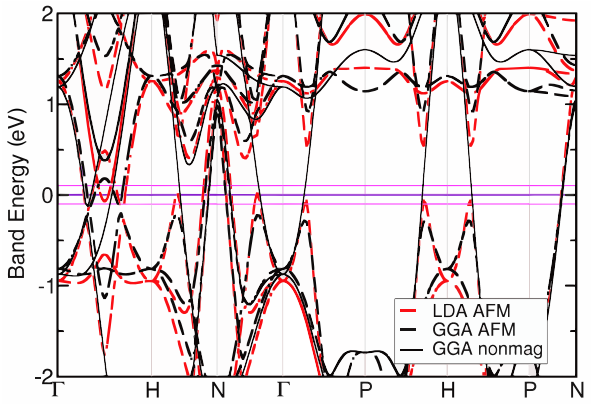

FIG. 1. Electron band structure of BCC Cr comparing non-magnetic and AFM ground states (the latter bands are folded due to the doubling of the unit cell from primitive to conventional cubic in AFM). Horizontal lines show E_F and a window of 0.1 eV.

The Brillouin zone was sampled in DFPT using a homogeneous grid of 16x16x16 k-points for electrons and 8x8x8 for phonons. We explored both non magnetic and

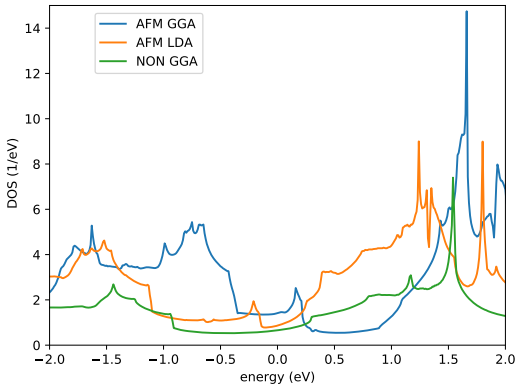

FIG. 2. Electron Density of States for BCC Cr comparing non-magnetic and AFM ground states, and LDA vs GGA. The AFM DOS is increased, and the band edges near the Fermi level give additional features which are crucial for EPC.

AFM ground states, using a weak magnetic constraint to guide the magnetic solution (see Ref.[6] for a discussion of exchange correlation effects in Cr). In GGA the AFM is more stable by only 1.5 mHa (in LDA less stable by 0.3 mHa), indicating a very close competition: spin fluctuations and other SDW/CDW ground states beyond AFM are known to occur in Chromium, and are very complex to simulate in DFT. The atomic magnetic moments (integrated in atomic spheres of radius 2 bohr) are 1.22 (GGA) and 0.60 (LDA) μ_B. The latter compares well with the SDW amplitude, as discussed by Cottenier as well, but is very sensitive to the lattice constant. Lattice constants used were 2.887 Å(GGA AFM) 2.848 Å(GGA non magnetic) and 2.800 Å(LDA AFM). The electron band structure near the Fermi level is shown in Fig. 1 (the bands for AFM are folded due to the conventional

supercell) and the DOS in 2. Several Fermi band crossings are removed by the AFM symmetry breaking, and the band positions also change critically when going from LDA to GGA, especially between Γ and H.

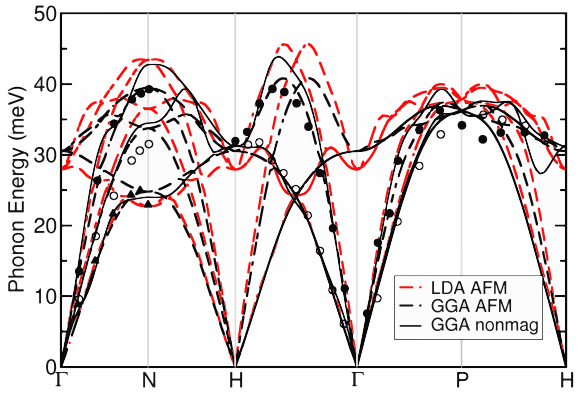

FIG. 3. Phonon band structure of BCC Cr compared to inelastic neutron scattering data extracted from [7].

The phonon band structure obtained is shown in figure 3 for AFM and non magnetic ground states, and comparing GGA with LDA. Agreement is quite good (average few percent error), in particular for the acoustic branches which are crucial to the present work, with the GGA AFM phonons closest to experiment.

ELECTRON PHONON COUPLING AND LIFETIMES

The electron phonon matrix elements were sampled on a denser 64x64x64 mesh, Fourier interpolating the perturbed DFPT potentials as proposed by Eiguren and Draxl [8], and integrated to obtain the electron phonon coupling strength λ and the phonon linewidths due to interaction with electrons (see e.g. [9]), as a function of wave vector q.

The LDA AFM exchange correlation produces harder phonons (this is common in LDA due to smaller relaxed volumes) but a very strong EPC with a total λ of 0.568 and $\lambda\langle\omega^2\rangle \sim 558$ mev^2, due to the additional bands crossing the Fermi level. The value of λ is close to the λ_{tr} extracted by Allen from transport data[10], but this may be a coincidence.

Using the calculated DOS and $\lambda\langle\omega^2\rangle$ we evaluate the expressions, in a 2 temperature model, for the total thermalization time τ_T as in Allen[10]

$$\frac{1}{\tau_T} = \left(3\hbar\lambda\langle\omega^2\rangle / \pi k_B T_e\right) \quad (1)$$

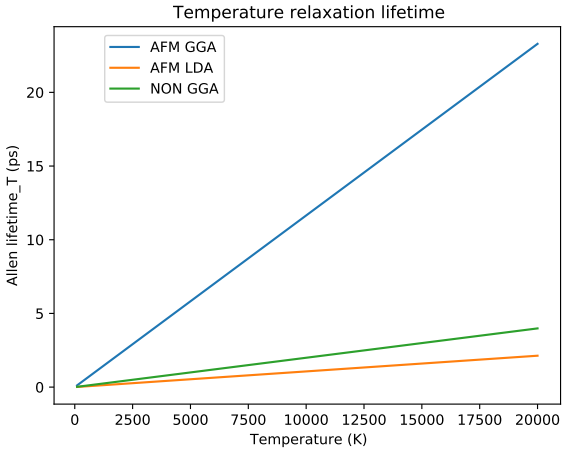

FIG. 4. Average thermalization times from the two temperature model by PB Allen, using the intrinsic DFPT $\lambda\langle\omega^2\rangle$.

and the total electron phonon coupling following Lin[11]:

$$G(T_e) = \frac{\pi\hbar k_B \lambda\langle\omega^2\rangle}{g(\varepsilon_F)} \int_{-\infty}^{\infty} g^2(\varepsilon)\left(-\frac{\partial f}{\partial\varepsilon}\right) d\varepsilon \quad (2)$$

where T_e is the electron temperature, ε an electron energy, $\lambda\langle\omega^2\rangle$ is the first moment of the Éliashberg spectral function, g is the DOS, and f the Fermi Dirac distribution. The results are shown in Figures 4 and 5: the EPC increases dramatically as the electron temperature is increased through laser heating, and the thermalization time is on the order of ps, as seen by Dresselhaus. Note that this approach loses the phonon mode and wavevector resolution, and integrates all phonons (most of which have very short lifetimes even at T=0K).

ANHARMONIC PHONON CALCULATIONS

The phonon-phonon TDEP calculations[12] were extracted from ab-initio molecular dynamics calculations using the VASP code [13, 14]. VASP relies on the projector augmented wave method (PAW) representation for the wave function, with an energy cutoff of 500 eV, and the same GGA functional used in the ABINIT calculations. A supercell of 250 atoms was employed, fitting forces to the interatomic force constants at 2nd (harmonic) and 3rd(anharmonic) orders, which are recalculated at each temperature (here only 300 Kelvin). The TDEP approach is very accurate as all higher order anharmonicities renormalize the explicit 2nd+3rd orders. The resulting phonon linewidths are an order of magnitude smaller than the EPC ones, and thus negligible for the discussion in the main text.

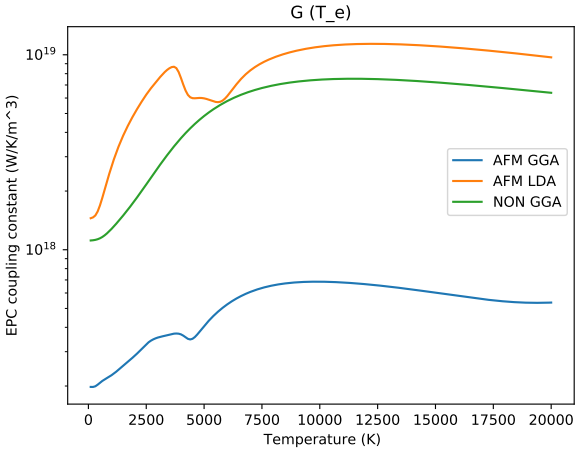

FIG. 5. Global averaged electron phonon coupling constant (log scale) as a function of electron temperature, using the approach of Lin et al., which incorporates the effect of realistic electron density of states, but leaves the intrinsic coupling unchanged. The ratio between AFM and non-magnetic solutions is the same, but increasing T to several thousand K increases G by almost a factor of 5-10.

* jcwingert@physics.ucsd.edu

[1] M. Verstraete and Z. Zanolli, in *Computing Solids: Models, Ab-initio Methods and Supercomputing, Lecture Notes of the 45th Spring School 2014*, Schlüsseltechnologien Key Technologies, Vol. 35, edited by S. Blügel, N. Helbig, V. Meden, and D. Wortmann, Forschungszentrum Jülich (Schriften des Forschungszentrums Jülich, Jülich, 2014) pp. C2.1 – C2.29.

[2] X. Gonze, F. Jollet, F. A. Araujo, D. Adams, B. Amadon, T. Applencourt, C. Audouze, J.-M. Beuken, J. Bieder, A. Bokhanchuk, E. Bousquet, F. Bruneval, D. Caliste, M. Côté, F. Dahm, F. Da Pieve, M. Delaveau, M. Di Gennaro, B. Dorado, C. Espejo, G. Geneste, L. Genovese, A. Gerossier, M. Giantomassi, Y. Gillet, D. R. Hamann, L. He, G. Jomard, J. Laflamme Janssen, S. L. Roux, A. Levitt, A. Lherbier, F. Liu, Lukacevic, A. Martin, C. Martins, M. J. T. Oliveira, S. Ponce, Y. Pouillon, T. Rangel, G. Rignanese, A. H. Romero, B. Rousseau, O. Rubel, A. A. Shukri, M. Stankovski, M. Torrent, M. J. van Setten, B. Van Troeye, M. J. Verstraete, D. Waroquier, J. Wiktor, B. Xu, A. Zhou, and J. W. Zwanziger, Comput. Phys. Commun. **205**, 106 (2016).

[3] D. R. Hamann, Phys. Rev. B **88**, 085117 (2013).

[4] M. van Setten, M. Giantomassi, E. Bousquet, M. Verstraete, D. Hamann, X. Gonze, and G.-M. Rignanese, Computer Physics Communications **226**, 39 (2018).

[5] J. P. Perdew, K. Burke, and M. Ernzerhof, Phys. Rev. Lett. **77**, 3865 (1996).

[6] S. Cottenier, B. D. Vries, J. Meersschaut, and M. Rots, Journal of Physics: Condensed Matter **14**, 3275 (2002).

[7] H. Møller and A. Makintosh, in *Inelastic Scattering of Neutrons* (IAEA, Vienna, 1965).

[8] A. Eiguren and C. Draxl, Phys. Rev. B **78**, 045124 (2008).

[9] F. Giustino, Rev Mod Phys **89**, 015003 (2017).

[10] P. B. Allen, Phys. Rev. B **36**, 2920 (1987).

[11] Z. Lin, L. V. Zhigilei, and V. Celli, Physical Review B **77**, 075133 (2008).

[12] O. Hellman, P. Steneteg, I. A. Abrikosov, and S. I. Simak, Physical Review B **87**, 104111 (2013).

[13] G. Kresse and J. Furthmüller, Phys. Rev. B **54**, 11169 (1996).

[14] G. Kresse and D. Joubert, Phys. Rev. B **59**, 1758 (1999).